Stability of RNA Hairpin Loops Closed by AU Base Pairs†

Christopher J. Vecenie and Martin J. Serra*

Department of Chemistry, Allegheny College, 520 North Main Street, Meadville, Pennsylvania 16335

Received January 6, 2004; Revised Manuscript Received July 1, 2004

ABSTRACT: Thermodynamic parameters are reported for hairpin formation in 1 M NaCl by RNA sequence of the type GCAXUAAUYUGC, where XY is the set of 10 possible mismatch base pairs. A nearest-neighbor analysis of the data indicates that the free energy of loop formation at 37 °C varies from 3.2 to 5.0 kcal/mol. These results combined with the model previously developed [Dale et al. (2000) *RNA 6,* 608] allow improvements in the model to predict the stability of RNA hairpin loops: $\Delta G^\circ_{37L(n)} = \Delta G^\circ_{37i(n)} + \Delta G^\circ_{37MM} - 0.8$ (if first mismatch is GA or UU) $- 0.8$ (if first mismatch is GG and loop is closed on 5′ side by a purine). Here, $\Delta G^\circ_{37i(n)}$ is the free energy for initiating a loop of *n* nucleotides, and ΔG°_{37MM} is the free energy for the interaction of the first mismatch with the closing base pair. Hairpins with GG first mismatches were found to vary in stability depending upon the orientation of the closing base pair (5′ or 3′ purine relative to the loop). The model gives good agreement when tested against four naturally occurring hairpin sequences.

RNA, like proteins, form specific secondary and tertiary structures in order to form biologically active molecules. RNAs are believed to rapidly form stable secondary structural elements that more slowly attain tertiary structural interactions for the active three-dimensional molecule. The folding of the single-stranded RNA molecule to form hairpins is believed to be one of the early events in RNA folding (*1*, *2*). Indeed, hairpins represent a large portion of the secondary structure observed in large RNAs. For example, the rRNAs are composed of approximately 70% small hairpin structures (*3*, *4*). Additionally, hairpins are involved in a number of important tertiary interactions with either proteins (*5*, *6*) or RNA (*7*, *8*). The ability of hairpins to form nucleation sites for further folding of RNA depends on the stability of the hairpin motif. Understanding the stability of RNA hairpins is therefore crucial to elucidating the folding pathway and ultimate three-dimensional structure of RNA.

Hairpin loop stability can be predicted using a relatively simple nearest-neighbor model (*9*−*12*). For hairpin loops larger than three, stability was shown to depend on the loop size, the interaction of the first mismatch with the closing base pair, and an additional stabilization term for loops with GA and UU first mismatches. The model was developed from a set of hairpins that were predominantly closed by CG with the cytosine residue to the 5′ side of the loop (nearly 50%; 34 or 71 hairpins with Watson−Crick base closures).

In this report, we investigate the influence of the closing base pair on the stability of RNA hairpin loops by examining the complete set of first mismatch with hairpins closed by AU (adenosine to the 5′ side of the loop). This set of hairpins not only switches from the more stable CG pair to the less stable AU pair but also switches the orientation of the purine and pyrimidine bases of the closing pair. The results of this study show that, for RNA hairpin loops, the orientation of the purine and pyrimidine bases of the closing base pair has a marked influence on the stability of the loops, in particular, for hairpins with GG first mismatches.

MATERIALS AND METHODS

RNA Synthesis and Purification. Oligomers were synthesized on solid support using the phosphoramidite approach with the 2′-hydroxyl protected as the *tert*-butyl dimethylsilyl ether. After ammonia and fluoride deprotection, the crude oligomer was purified by preparative TLC (1-propanol: ammonium hydroxide:water, 55:35:10) and Sep-Pak C18 (Waters) chromatography. Purities were checked by analytical TLC and were greater than 95%.

Melting Curves and Data Analysis. The buffer for the melting studies was 1 M NaCl, 10 mM cacodylic acid, and 0.5 mM EDTA, pH 7. Strand concentrations were determined from high-temperature absorbance at 280 nm. Absorbance versus temperature curves were measured at 280 or 260 nm, with a heating or cooling rate of 1.0 °C min^{-1}, on a Perkin-Elmer Lambda 2S spectrophotometer as described previously (*12*). Oligomer concentrations were varied over at least a 40-fold range between 1 mM and 10 μM.

Absorbance versus temperature profiles were fit to a two-state model with sloping baselines by using a nonlinear least-squares program (*13*). For hairpin melts, this program was adapted for a unimolecular transition. Thermodynamic parameters for hairpin formation were obtained from averages of the fits of the individual melting curves. The melting temperatures for all of the hairpins were concentration independent, indicative of a unimolecular transition. Thermodynamic parameters for duplex formation were obtained by two methods: (1) enthalpy and entropy changes from the fits of the individual melting curves were averaged, and

† This work was supported by the Camille and Henry Dreyfus Foundation, National Science Foundation, and Shambron Funds of Allegheny College.

* To whom correspondence should be addressed. Phone: 814-332-5356. Fax: 814-332-2789. E-mail: mserra@allegheny.edu.

10.1021/bi049954i CCC: $27.50
Published on Web 08/25/2004

Table 1: Thermodynamic Parameters for Hairpin Formation at 1 M NaCl[a]

A A
U U
X Y
A•U
C•G
G•C

XY	T_M (°C)	$\Delta H°$ (kcal/mol)	$\Delta S°$ (eu)	$\Delta G°_{37}$ (kcal/mol)	$\Delta G°_{37L}$[b] measd (pred) (kcal/mol)
GA	51.6	−39.4 ± 3.8	−120.9 ± 11.5	−1.87 ± 0.26	3.2 (3.8)
UU	49.5	−40.3 ± 3.8	−125.0 ± 11.9	−1.57 ± 0.33	3.5 (3.9)
GG	57.8	−25.0 ± 1.8	−75.6 ± 5.7	−1.57 ± 0.28	3.5 (3.7)
AG	47.3	−22.7 ± 2.0	−70.9 ± 6.7	−0.73 ± 0.18	4.4 (4.8)
UC	42.9	−29.2 ± 1.7	−92.4 ± 5.3	−0.55 ± 0.06	4.5 (4.9)
CC	43.1	−26.6 ± 2.5	−84.2 ± 7.4	−0.51 ± 0.21	4.6 (4.7)
AC	44.9	−19.8 ± 1.8	−62.3 ± 5.3	−0.49 ± 0.17	4.6 (4.7)
AA	42.6	−23.6 ± 1.8	−74.8 ± 6.0	−0.42 ± 0.03	4.7 (4.6)
CA	40.6	−23.5 ± 1.8	−74.8 ± 5.7	−0.27 ± 0.17	4.8 (4.8)
CU	38.9	−18.9 ± 1.6	−60.5 ± 5.3	−0.12 ± 0.15	5.0 (5.2)

[a] Solutions are 1 M NaCl, 10 mM sodium cacodylate, and 0.5 mM EDTA, pH 7. [b] Calculated $\Delta G°_{37L} = \Delta G°_{37(\text{measured for hairpin formation})} - \Delta G°_{37(\text{stem})}$.

(2) plots of the reciprocal melting temperature, T_M^{-1}, versus log C_t gave enthalpy and entropy changes (*14*):

$$T_M^{-1} = (2.3R/\Delta H°) \log C_t + \Delta S°/\Delta H° \quad (1)$$

Here, C_t is the total concentration of oligomer. Parameters derived from the two methods agreed within 10%, consistent with the two-state model.

RESULTS

We have previously shown that, for RNA hairpin loops closed by a CG base pair, the stability of the hairpin is dependent upon the interaction of the closing base pair with the first mismatch (*12*). This interaction can be approximated by the free energy increment for the interaction of mismatch at the end of a duplex, $\Delta G°_{37MM}$. Hairpins with GA or UU first mismatches were unusually stable, and to model the stability of these hairpin loops, an additional stabilization term (0.8 kcal/mol) was included. To more fully determine the role of the first mismatch on the stability of hairpin loops, a complete set of hairpins with AU pairs, but differing in the first mismatch, were prepared and the thermodynamics of hairpin formation measured by optical melting. In this study, we chose not only to switch from a more stable CG to less stable AU closure but also to switch the positions of the purine and pyrimidine bases (CG, purine is located 3′; AU, purine is located 5′ of the hairpin loop).

The measured thermodynamic parameters for the hairpins with the 10 different first mismatches are listed in Table 1. The free energy change for hairpin formation $\Delta G°_{37}$ varies from −1.8 to −0.1 kcal/mol. The stability of an RNA hairpin can be dissected into its two structural motifs, the double helical stem and loop. The free energy contribution of the loop can be determined by

$$\Delta G°_{37L} = \Delta G°_{37(\text{measured for hairpin formation})} - \Delta G°_{37(\text{stem})} \quad (2)$$

Since all of the hairpins contain a common stem 5′GCA/CGU ($\Delta G°_{37} = -5.08$ kcal/mol) calculated according to ref *15*, the free energy for loop formation varies by an amount equivalent to the difference in hairpin stability. The results of this analysis are presented in Table 1.

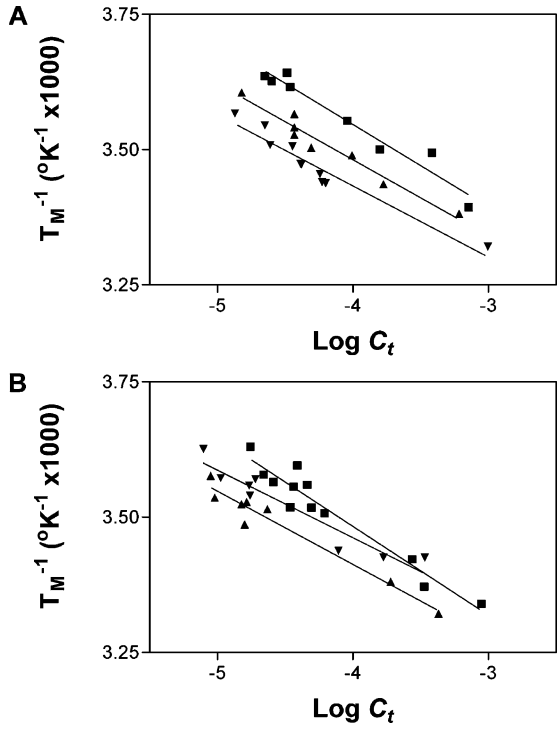

FIGURE 1: Reciprocal melting temperature versus log concentration plots:. (A) (■) UUCGAC, (▲) GUCGAA, and (▼) UUCGAU and (B) (■) CUCGAA, (▼) CUCGAU, and (▲) GUCGAG in 1 M NaCl, 10 mM sodium cacodylate, and 0.5 mM EDTA, pH 7.

We have previously shown (*11*, *12*) that the stability of hairpin loops closed by Watson−Crick base pairs larger than three could be modeled using the simple equation:

$$\Delta G°_{37L(n)} = \Delta G°_{37i\,(n)} + \Delta G°_{37MM} - 0.8 \quad \text{(if first mismatch is GA or UU)} \quad (3)$$

Here, $\Delta G°_{37i(n)}$ is the free energy for initiating a loop of n nucleotides and $\Delta G°_{37MM}$ is the free energy for stacking of the first mismatch on the closing base pair. The $\Delta G°_{37MM}$ is approximated by the free energy of stacking the mismatches at the ends of helices. The model was derived primarily from a set of hairpins with CG closing base pairs (*12*). To determine if a similar equation can be used for predicting the stability of hairpin loops closed by AU base pairs, the $\Delta G°_{37MM}$ for helices ending in an AU base pair must be known. The thermodynamic parameters for only three terminal mismatches (AA, CA, and GA) on helices ending in AU have been determined (ref *16* and references cited therein). Therefore, several mismatches (XY) on an AU base pair were measured using self-complementary oligomers of the type YUCGAX. Plots of T_M^{-1} vs log C_t are shown in Figure 1, and the thermodynamic parameters are presented in Table 2. The T_M^{-1} vs log C_t plots are more scattered than usual because of the low melting temperatures of the oligomers and the difficulty in fitting the lower baselines. However, there is excellent agreement between the thermodynamic parameters determined from the fit of the melt curves and the plots of $1/T_M^{-1}$ vs log C_t. The nearest-neighbor thermodynamic parameters for the terminal mismatches on

Table 2: Thermodynamic Parameters of Duplex Formation[a]

	T_M^{-1} vs log C_t plots				average curve fits			
sequence	$-\Delta H°$ (kcal/mol)	$-\Delta S°$ (eu)	$-\Delta G_{37}°$ (kcal/mol)	T_M[b] (°C)	$-\Delta H°$ (kcal/mol)	$-\Delta S°$ (eu)	$-\Delta G_{37}°$ (kcal/mol)	T_M[b] (°C)
CUCGAA	27.96 ± 2.4	79.01 ± 8.5	3.45 ± 0.2	14.1	27.86 ± 2.5	78.59 ± 8.3	3.48 ± 0.2	14.3
GUCGAA	32.63 ± 2.9	95.24 ± 10.2	3.09 ± 0.3	14.2	28.38 ± 2.1	80.35 ± 6.9	3.46 ± 0.2	14.6
UUCGAC	30.16 ± 2.8	88.60 ± 10.1	2.68 ± 0.3	9.0	34.44 ± 2.6	103.73 ± 8.6	2.26 ± 0.2	9.0
GUCGAG	33.78 ± 2.9	96.93 ± 10.2	3.72 ± 0.3	20.0	31.24 ± 2.8	87.95 ± 9.4	3.96 ± 0.2	20.9
CUCGAU	36.64 ± 4.6	108.49 ± 16.3	2.99 ± 0.5	15.9	36.38 ± 3.0	107.56 ± 11.2	3.02 ± 0.5	15.9
UUCGAU	34.86 ± 3.4	101.29 ± 11.7	3.44 ± 0.3	18.3	32.19 ± 2.2	92.05 ± 7.9	3.64 ± 0.3	18.6
reference duplex UCGA[c]	24.47	72.2	2.07					

[a] Solutions are 1 M NaCl, 10 mM sodium cacodylate, and 0.5 mM EDTA, pH 7. [b] Calculated at 10^{-4} M oligomer concentration. [c] Predicted (*15*).

Table 3: Thermodynamic Parameters for Terminal Mismatches on an AU Pair (1 M NaCl)[a]

$\rightarrow$ AX UY $\leftarrow$

	Y			
X	A	C	G	U
		$-\Delta H°$ (kcal/mol)		
A	3.9	1.8	4.08	
C	2.3	(6.0)		2.9
G	3.1		4.7	
U		6.09		5.2
		$-\Delta S°$ (eu)		
A	10.2	3.4	1.2	
C	5.3	(21.6)		8.2
G	7.3		12.4	
U		18.1		14.6
		$-\Delta G°_{37}$ (kcal/mol)		
A	0.8	0.7	0.6	
C	0.6	(0.7)		0.2
G	0.8		0.9	
U		0.5		0.7

[a] $\Delta G°_{37}$'s calculated as illustrated in the text. Values in parentheses are estimated.

an AU base pair are derived from equations equivalent to (*17*)

$$\Delta G°\left(\begin{smallmatrix}\mathrm{AX}\\ \mathrm{UY}\end{smallmatrix}\right) = 0.5[\Delta G°(\mathrm{YUCGAX}) - \Delta G°(\mathrm{UCGA})] \quad (4)$$

Table 3 summarizes these parameters. The measured $\Delta G°_{37}$ values for the terminal mismatches are close (within 0.5 kcal/mol) to the predicted values (*16*) for all of the duplexes.

Figure 2 shows a plot of the free energy for hairpin loop formation, $\Delta G°_{37L}$, versus the free energy increment of the first mismatch in the loop for the 10 hairpins closed by AU and the 10 hairpins closed by CG (*12*) base pairs. The trend observed for hairpins closed by CG, where the loops with more stable first mismatches are more stable, is also true for hairpins closed by AU base pairs. For hairpin loops closed by CG base pairs, loops with first mismatches of GA and UU were shown to be more stable (*12*). For hairpins closed by AU base pairs, there are three loops which display unusual stability. In addition to first mismatches of GA and UU, the GG first mismatch is also more stable than other hairpin loops. When the unusually stable mismatches (labeled in Figure 2) are omitted, a linear fit to the data in Figure 2 gives $\Delta G°_{37L(6)} = 5.2 + \Delta G°_{37MM}$ ($r = 0.78$; slope -0.92 ± 0.14), where $\Delta G°_{37MM}$ is the free energy increment for the first mismatch in the loop as measured at duplex ends. The 5.2 for $\Delta G°_{37L(6)}$ is close to the $\Delta G°_{37i\ (6)}$ of 5.4 determined from the average of all measured hairpin loops of six (ref *16* and references cited therein).

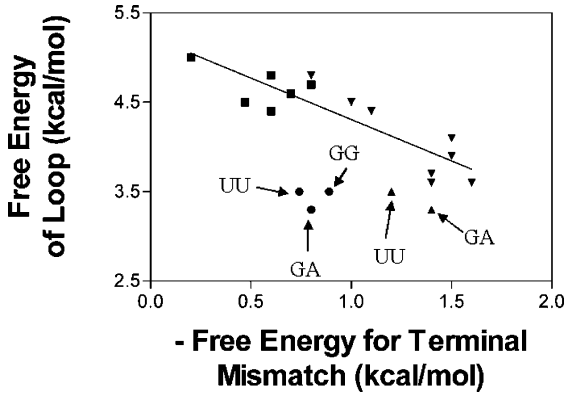

FIGURE 2: Plot of free energy change for hairpin loop formation. $\Delta G°_{37L}$ versus the free energy increment $\Delta G°_{37MM}$ for the first mismatch of the loop. Loops are closed by (▲, ▼) CG or (■, ●) AU. Unusually stable first mismatches are labeled in the figure. The solid line is the least-squares fit to the data points, excluding the unusually stable first mismatches.

To test the generality of the conclusions from this work, thermodynamic parameters were also measured for four hairpins of six nucleotides that occur naturally in the small or large rRNAs. These results are listed in Table 4.

DISCUSSION

The trend in terms of stability of the hairpins examined here, closed by AU base pairs, parallels the trend in stability for hairpins closed by CG base pairs. The order of stability for the hairpins closed by an AU base pair and the previously measured hairpin closed by CG (*12*) is nearly identical. The only hairpins that occur in a different order of stability for the two sets of hairpins are those with first mismatches of AA, UC, AC, and CC. They are the fifth to eighth most stable in both sets, but the order differs for the two sets. The difference in order of stability may reflect the very small differences in stability among the hairpins in this study (<0.1 kcal/mol), clearly within experimental error.

The most striking difference in the two sets of data was the stability of the hairpins with GG first mismatches, while, in both sets, the GG hairpin was the third most stable hairpin, following GA and UU. For hairpins closed by CG the stability of the GG first mismatch could be modeled as having normal stability, while for the AU closed hairpin,

Table 4: Thermodynamic Parameters for Hairpin Formation of Natural Sequences in 1 M NaCl[a]

RNA Hairpin			T_M (°C)	ΔH° (kcal/mol)	ΔS° (eu)	$\Delta G°_{37}$ (kcal/mol)	$\Delta G°_{37L}$[b] (kcal/mol)
UU							
GCA	A	*c*	50.5	-27.9 ± 3.2	-86.14 ± 10.3	-1.16 ± 0.28	3.9
CGU	A		(50.4)	(-27.6)	(-85.3)	(-1.2)	(3.9)[b]
UG							
UA							
GCA	U	*d*	47.4	-43.2 ± 3.1	-134.6 ± 9.4	-1.40 ± 0.37	3.7
CGU	G		(50.4)	(-27.6)	(-85.3)	(-1.2)	(3.9)
UU							
GU							
GCA	U	*e*	57.3	-21.8 ± 1.7	-66.05 ± 5.7	-1.34 ± 0.28	3.7
CGU	A		(53.0)	(-27.1)	(-83.1)	(-1.4)	(3.7)
GU							
GA							
GCA	A	*f*	43.7	-21.2 ± 2.0	-66.89 ± 6.8	-0.45 ± .43	4.6
CGU	U		(53.0)	(-27.1)	(-83.1)	(-1.4)	(3.7)
GA							

[a] Solutions are 1 M NaCl, 10 mM sodium cacodylate, and 0.5 mM EDTA, pH 7. [b] Calculated as described in the text. [c] Sequence modeled on *Bacillus anthracis* small subunit rRNA position 1135. [d] *Bordetella bronchiseptica* large subunit rRNA position 567. [e] *Staphylococcus aureus* large subunit rRNA position 138. [f] *B. anthracis* large subunit rRNA position 955 [*E. coli* equivalent positions (*3*)]. Values in parentheses are predicted.

Table 5: Summary of Hairpin Loops with GG First Mismatch Stability[a]

RNA Hairpin	$\Delta G°_{37}$ kcal/mol (Pred.)[b]	$\Delta G°_{37i}$[b] kcal/mol (Pred.)[b]	$\Delta G°_{37\,MM}$ kcal/mol	$\Delta G°_{37Li}$[b] kcal/mol
5' pyrimidine				
GGCGUAAUGGCC[c]	-3.1 (-2.9)	+3.6 (+3.8)	-1.6	+5.2
GGUGUAAUGACC[c]	-1.0 (-0.8)	+4.0 (+4.2)	-1.2	+5.2
GGUGUAAUGGCC[d]	-1.3 (-0.7)	+4.0 (+4.6)	-0.8	+4.8
GGUGUAAUGACC[e]	-1.0 (-0.9)	+4.1 (+4.2)	-1.2	+5.3
Average				+5.1
5' purine				
GCGGUAAUGCGC[e]	-2.5 (-2.6)	+3.3 (+3.2)	-1.4	+4.7
GGAGUAAUGUCC[e]	-1.2 (-1.5)	+4.0 (+3.7)	-0.9	+4.9
GCGGUAAUGUGC[e]	-0.8 (-0.6)	+3.6 (+3.8)	-0.8	+4.4
GCAGUAAUGUGC[f]	-1.6 (-1.4)	+3.5 (+3.7)	-0.9	+4.4
GCAGUUAUGUGC[f]	-1.3 (-1.4)	+3.5 (+3.7)	-0.9	+4.4
GCAGAAUAGUGC[f]	-0.4 (-1.4)	+4.6 (+3.7)	-0.9	+5.5
Average				+4.7

[a] Solutions are 1 M NaCl, 10 mM sodium cacodylate, and 0.5 mM EDTA, pH 7. [b] Calculated as described in the text. [c] Reference *12*. [d] Reference *10*. [e] Reference *11*. [f] This study.

the GG first mismatch is unusually stable, being 0.9 kcal/mol more stable than expected. The unusual stability of hairpin loops with GG first mismatches with hairpins closed by AU base pairs is not totally unexpected. In some contexts [1 × 1 and 2 × 2 internal loops (*18*, *19*)] GG is more stable by more than 2 kcal/mol relative to other mismatches, while in other contexts [terminal mismatches (*15*)], GG has nearly the same stability as other mismatches.

The hairpins with GG first mismatches from this study were combined with GG first mismatch hairpins that had been previously studied (*10*−*12*) and are presented in Table 5. The stability of the hairpin loops ($\Delta G°_{37i}$) could be grouped into two classes, the first were the less stable (+4.8−5.2) and the second were the more stable (+4.4−4.8). The less stable group had the pyrimidine from the closing base pair to the 5′ side of the loop. The more stable group had the purine of the closing base pair to the 5′ side of the loop. The average $\Delta G°_{37i}$ for the hairpins with the pyrimidine to the 5′ side of the loop had an average value of +5.1 kcal/mol, not significantly different than the +5.4 kcal/mol value currently used to predict the stability of RNA hairpin loops of six nucleotides (*16*). For the hairpin loops with the purine base to the 5′ side of the loop, one hairpin is less stable than the others (GGAGAAUAGUGC). It is possible that the stability of this hairpin is different than the rest since it is the only hairpin that does not have a uracil residue as the second nucleotide of the loop. The structure of RNA hairpin loops of six has shown this base to be involved in a U-turn motif (*20*). The lack of uracil at this position may cause the loop to adapt an alternate, less favorable geometry. Even including this hairpin, the results do not change significantly; the hairpin loops with the purine of the closing base pair are more stable. The average stability of the hairpin loops without including the GGAGAAUAGUGC hairpin is +4.6 (+4.7 with its inclusion). Excluding this hairpin, the two sets of stabilities are significantly different from each other. Therefore, hairpins with GG first mismatches and the purine nucleotide of the closing base pair to the 5′ side of the loop are modeled as more stable than previously predicted by 0.8 kcal/mol. Combining this result with the previous model for the prediction of RNA hairpin stability leads to the model:

$$\Delta G°_{37L(n)}\ (\text{kcal/mol}) = \Delta G°_{37i(n)} + \Delta G°_{37MM} - 0.8\ (\text{if first mismatch is GA or UU}) - 0.8\ (\text{if first mismatch is GG and the loop is closed on the 5′ side by a purine}) \quad (5)$$

The above model was used to predict the $\Delta G°_{37iL}$ for the sequences listed in Tables 1 and 4, and the predicted values are listed in parentheses. Most sequences are predicted within 0.3 kcal/mol. The hairpin loop closed by AU with a GA first mismatch is 0.6 kcal/mol more stable than predicted (Table 1). Although this agreement is not as good as for other hairpin loops, it is still not bad, considering the simplicity of the model. The other sequence not predicted well by the model is the sequence GCAGAAUAGUGC, which is less stable than predicted by 0.9 kcal/mol (Table 5). As discussed above, the lower stability of this hairpin may be due to the lack of a uracil residue on the 5′ side of the loop that would allow a U-turn motif in the loop (*21*, *22*). Most of the hairpins used to develop the current model (*12*, *23*) had a uracil residue at the second position of the loop so more hairpins without the potential to form a U-turn motif will need to be investigated to determine the influence of this position on hairpin loop stability. The differences determined here for the stability of hairpin loops closed by different base pairs suggest that it would be useful to examine the complete set of closing base pairs and first mismatch combinations and the influence of the second position of the loop.

An examination of 692 hairpin loops of six found in the large and small ribosomal subunit RNAs (*3*,*4*) reveals that little more that half (51%) of the loops are closed with the purine base to the 5′ side of the loop. These loops have a

smaller percentage of GG first mismatches than those loops with a pyrimidine base to the 5′ side of the loop. This suggests that these loops were not selected for their stability.

ACKNOWLEDGMENT

We thank Douglas H. Turner for careful reading of the manuscript and many stimulating discussions.

REFERENCES

1. Hinz, H.-J., Filimonov, V. V., and Privalov, P. L. (1977) Calorimetric studies on melting of tRNA Phe (yeast), *Eur. J. Biochem. 72*, 79−86.
2. Privalov, P. L., and Filamonov, V. V. (1978) Thermodynamic analysis of transfer RNA unfolding, *J. Mol. Biol. 122*, 447−464.
3. Gutell, R. R., Gray, M. W., and Schare, M. N. (1993) A compilation of large subunit (23S and 23S-like) ribosomal RNA structures, *Nucleic Acids Res. 21*, 3055−3074.
4. Gutell, R. R. (1994) Collection of small subunit (16S and 16S-like) ribosomal subunit RNA structures, *Nucleic Acids Res. 22*, 3502−3507.
5. Wu, H. N., and Uhlenbeck, O. C. (1987) Role of a bulged A residue in a specific RNA-protein interaction, *Biochemistry 26*, 8221−8227.
6. Lazinski, D., Grzadzielska, E., and Das, A. (1989) Sequence-specific recognition of RNA hairpins by bacteriophage antiterminators requires a conserved arginine-rich motif, *Cell 59*, 207−218.
7. Murphry, F. L., Wang, Y., Griffith, J. D., and Cech, T. R. (1994) Coaxially stacked RNA helices in the catalytic center of the Tetrahymena ribozyme, *Science 265*, 1709−1712.
8. Marino, J. P., Gregorian, R. S., Jr., Csankovski, G., and Crothers, D. M. (1995) Bent helix formation between RNA hairpins with complementary loops, *Science 268*, 1448−1454.
9. Serra, M. J., Barnes, T. W., Betschart, K., Gutierrez, M. J., Sprouse, K. J., Riley, C. K., Stewart, L., and Temel, R. E. (1997) Improved parameters for the prediction of RNA hairpin stability, *Biochemistry 36*, 4844−4851.
10. Giese, M. R., Beschart, K., Dale, T., Riley, C. K., Rowan, C., Sprouse, K. J., and Serra, M. J. (1998) Stability of RNA hairpins closed by wobble base pairs, *Biochemistry 37*, 1094−1100.
11. Dale, T., Smith, R., and Serra, M. J. (2000) A test of the model to predict unusually stable RNA hairpin loop stability, *RNA 6*, 608−615.
12. Serra, M. J., Axenson, T. J., and Turner, D. H. (1994) A model for the stabilities of RNA hairpins based on a study of the sequence dependence of stability for hairpins with six nucleotides, *Biochemistry 33*, 14289−14296.
13. McDowell, J. A., and Turner, D. H. (1996) Investigation of the structural basis for thermodynamic stabilities of tandem GU mismatches: Solution structure of (rGAGGUCUC)$_2$ by two-dimensional NMR and simulated annealing, *Biochemistry 35*, 14077−14089.
14. Borer, P., Dengler, B., and Tinoco, I., Jr. (1974) Stability of ribonucleic acid double-stranded helices, *J. Mol. Biol. 86*, 843−853.
15. Xia, T., SantaLucia, J., Jr., Burkard, M. E., Kierzek, R., Schroeder, S., Jiao, X., Cox, C., and Turner, D. H. (1998) Thermodynamic parameters for an expanded nearest-neighbor model for formation of RNA duplexes with Watson−Crick base pairs, *Biochemistry 37*, 14719−14735.
16. Mathews, D. H., Sabina, J., Zuker, M., and Turner, D. H. (1999) Expanded sequence dependence of thermodynamic parameters improves prediction of RNA secondary structure, *J. Mol. Biol. 288*, 911−940.
17. Hickey, D. R., and Turner, D. H. (1985) Effects of terminal mismatches on RNA stability: Thermodynamics of duplex formation for ACCGGGp, ACCGGAp, and ACCGGCp, *Biochemistry 24*, 3987−3991.
18. Kierzek, R., Burkard, M., and Turner, D. H. (1999) Thermodynamics of single mismatches in RNA duplexes, *Biochemistry 38*, 14214−14223.
19. Burkard, M. E., Xia, T., and Turner, D. H. (2001) Thermodynamics of RNA internal loops with a guanosine-guanosine pair adjacent to another noncanonical pair, *Biochemistry 40*, 2478−2483.
20. Fountain, M. A., Serra, M. J., Krugh, T. R., and Turner, D. H. (1996) Structural features of a six-nucleotide RNA hairpin loop found in ribosomal RNA, *Biochemistry 35*, 6539−6548.
21. Quigley, G. J., and Rich, A. (1976) Structural domains in transfer RNA molecules. The ribose 2′ hydroxyl which distinguishes RNA from DNA plays a key role in stabilizing tRNA structure, *Science 194*, 796−806.
22. Juker, F. M., and Pardi, A. (1995) GNRA tetraloops make a U-turn, *RNA 1*, 219−222.
23. Serra, M. J., Little, M. H., Axenson, T. J., Schadt, C. A., and Turner, D. H. (1993) RNA hairpin loop stability depends on closing base pair, *Nucleic Acids Res. 21*, 3845−3849.

BI049954I